

Metamaterial polarizers by electric-field-coupled resonators

Jessie Y. Chin, Mingzhi Lu, and Tie Jun Cui^{a)}

State Key Laboratory of Millimeter Waves, Southeast University, Nanjing 210096, Republic of China

(Received 23 September 2008; accepted 1 December 2008; published online 22 December 2008)

The idea of transmission polarizers realized by anisotropic metamaterials is demonstrated by experiments. One of the polarizers converts linear-polarized waves to circular-polarized waves, while the other polarizer converts linear-polarized waves from one polarization to its cross polarization. The excellent agreement between experimental results and theoretical predictions validates the functions and efficiency of the proposed polarizers. © 2008 American Institute of Physics. [DOI: 10.1063/1.3054161]

Metamaterials have opened up an access to counterintuitive material parameters, accurate control over the distribution of material parameters, and designable anisotropy of the materials.¹⁻³ Previously, there have been reports on metamaterial slabs with anisotropic material parameters manipulating polarization status.^{4,5} Polarization, as a property of transverse waves, has found widespread applications including liquid crystal display, radio frequency antenna radiation, satellite communication, and optical instrumentation. Conventionally, polarizers allow a single polarization state by reflecting the unwanted state or by splitting mixed-polarization waves into two wave beams with perpendicular polarizations. Therefore, one wave beam carries less than half of the total incident energy.

In this letter, we propose the idea of transmission polarizer by an anisotropic metamaterial slab, in which the function and the transmission efficiency of the polarizer can be designably controlled. The metamaterial polarizer is further simulated and fabricated based on the electric inductance-capacitance (ELC) resonator particle, which has a strong coupling with local electric field and shows an designable effective electric permittivity.^{6,7} Among the differently shaped ELC particles investigated in Ref. 7, the ELC with two pairs of arms shown in Fig. 1(a) is adopted for its anisotropic material response and merit of being electrically small. The transmission polarizer has favorable advantages of little absorption and small reflections. Compared to the reflector polarizer,⁴ the incoming and outgoing waves are naturally well separated, and therefore do not interfere with each other. Measurement results are shown for the cases of linear-to-circular polarization conversion and linear-to-linear polarization conversion.

As pointed out in the theoretical analysis,⁵ under normal incidence, waves propagating in an anisotropic metamaterial slab along the z -axis can be decomposed into two modes with the electric fields along the x -axis and the y -axis, respectively. For the two wave modes, the transmission coefficients T^x and T^y are related to the metamaterial effective material properties by

$$T^{x,y} = \frac{\exp(ik_{x,y}d) - r_{x,y}^2 \exp(ik_{x,y}d)}{1 - r_{x,y}^2 \exp(2ik_{x,y}d)}, \quad (1)$$

in which d is the thickness of the metamaterial slab, $k_{x,y}$ is the wave number for the two wave modes, and $r_{x,y}$ is the reflection coefficient at the air-metamaterial interface,

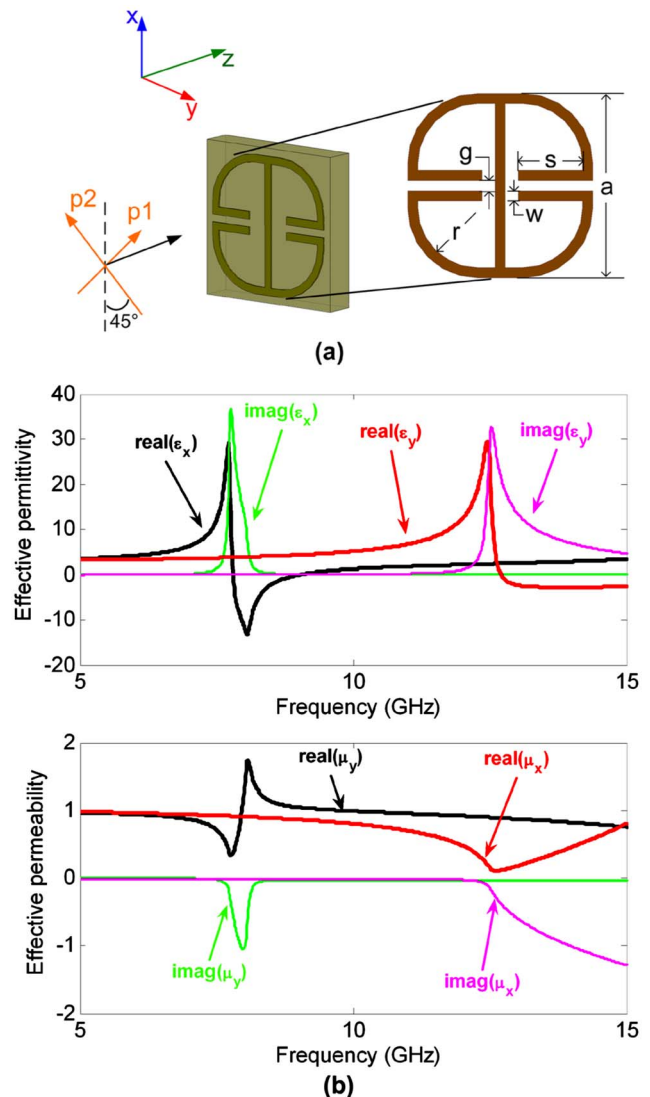


FIG. 1. (Color online) (a) The ELC simulated and its geometry design: $a=3.6$ mm, $w=0.2$ mm, $g=0.2$ mm, and s and r are variables. The copper thickness is 0.035 mm and the substrate thickness is 0.75 mm. (b) The anisotropic permittivity and permeability of the optimized ELC from 5 to 15 GHz.

^{a)}Electronic mail: tjcui@seu.edu.cn.

$$r_{x,y} = \frac{\eta_0 - \eta_{x,y}}{\eta_0 + \eta_{x,y}}, \quad (2)$$

where η_0 is the wave impedance of air and $\eta_{x,y}$ is the wave impedance of the metamaterial slab for the two wave modes.

Given a transverse electromagnetic incident wave with electric field $\vec{E} = \hat{x}E_x + \hat{y}E_y$, the conditions for linear outgoing waves are derived as

$$|E_x| \cdot |T^x| = p|E_y| \cdot |T^y|, \quad (3)$$

$$[\arg(E_x) + \arg(T^x)] - [\arg(E_y) + \arg(T^y)] = k\pi, \quad (4)$$

where $k=0, \pm 1, \pm 2, \pm 3, \dots$, and p decides the orientation of the electric field ($0 \leq p \leq 1$). The conditions for elliptical outgoing waves are

$$|E_x| \cdot |T^x| = q|E_y| \cdot |T^y|, \quad (5)$$

$$[\arg(E_x) + \arg(T^x)] - [\arg(E_y) + \arg(T^y)] = \frac{k\pi}{2}, \quad (6)$$

where q is the minor to major ratio of the polarization ellipse. When $q=1$, the elliptical polarization becomes circular polarization. By designing the material parameters of the metamaterial slab, we are able to control the values of T^x and T^y . By controlling the orientation of the slab with respect to the polarization of the incident waves, we are able to adjust $|E_x|/|E_y|$. And if we tune the transmission coefficients T^x and T^y as close to 0 dB as possible, the metamaterial polarizer will have a high overall transmission coefficient. Thus the linear polarization can be efficiently rotated by an arbitrary angle and waves can be switched between any elliptical polarizations or circular polarizations with little loss of energy.

To demonstrate the idea of the transmission polarizer, we choose the instances of converting a linear polarization to a circular polarization and to its cross linear polarization. If the incident waves are linearly polarized as $|E_x|=|E_y|$ and $\arg(E_x)=\arg(E_y)$, while T^x and T^y have the following relations

$$|T^x| = |T^y|, \quad (7)$$

$$\arg(T^x) - \arg(T^y) = -\frac{3\pi}{2}, \quad (8)$$

Eqs. (5) and (6) will be satisfied with $q=1$ and the outgoing waves will be circularly polarized. If we are able to control $|T^x|$ and $|T^y|$ to be close to 0 dB, nearly all the energy will be transmitted to the targeted polarization.

For four layers of the same ELC structures, we therefore have $|T^x|=|T^y|$ and $\arg(T^x) - \arg(T^y) = -3\pi$, which means that with the same linear incident waves, the metamaterial slab will polarize the waves to its cross linear polarization.

We used the commercial software ANSOFT HFSS to simulate a $4 \times 4 \times 4$ mm³ ELC particle shown in Fig. 1(a), in which the F4B substrate has a relative permittivity of 3.0 + $i0.01$. We first simulated S -parameters of ELC with electric boundary condition along the x -axis and magnetic boundary condition along the y -axis in order to achieve the effective permittivity ϵ_x and permeability μ_y by the retrieval technique introduced in Ref. 8. We are then, by Eq. (1), able to calculate T^x for ELC metamaterial slab with different thicknesses. Likewise, ϵ_y , μ_x , and T^y can be calculated from simulated

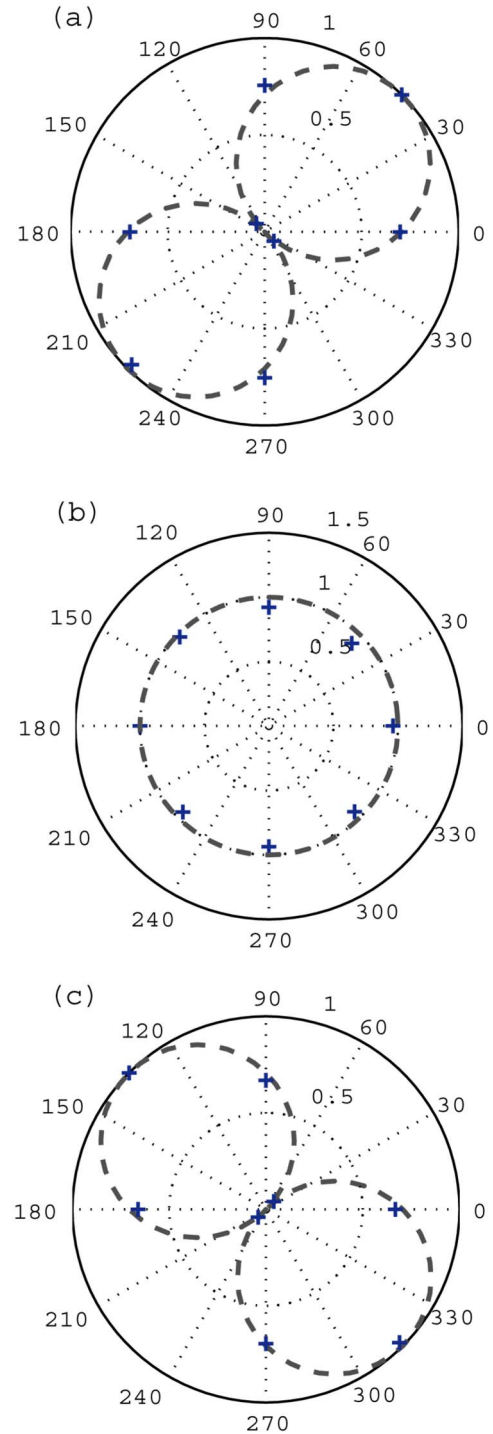


FIG. 2. (Color online) The theoretical polarization patterns (dotted lines) and the measured polarization patterns (plus signs) of the (a) incident waves, (b) transmitted waves through the two-layer ELC sample, and (c) transmitted waves through the four-layer ELC sample.

S -parameter with electric boundary condition along the y -axis and magnetic boundary condition along the x -axis. By changing the geometry parameters s and r , we searched through the available values of T^x and T^y at 9.5 GHz for one up to three layers of ELC, and eventually we optimized T^x and T^y to match the relations of Eqs. (7) and (8) in the case of two-layer ELC. The optimized geometry parameters are $s=0.99$ mm and $r=1.18$ mm while T^x and T^y are kept to be greater than -1 dB. Retrieved anisotropic permittivity and permeability are plotted in Fig. 1(b).

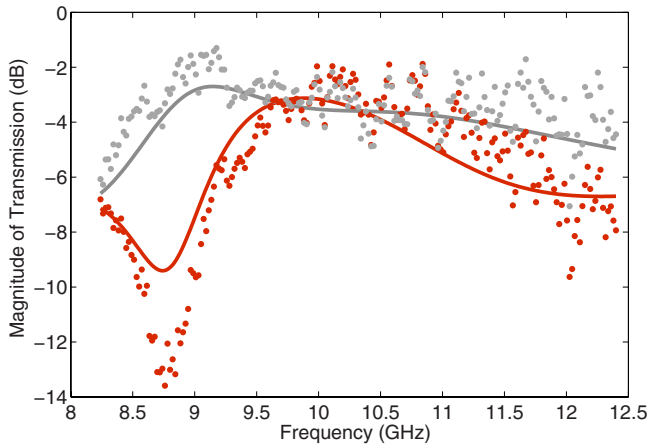


FIG. 3. (Color online) The simulated (solid lines) and measured (dots) transmission of electric field from p1 to p1 (gray) and from p1 to p2 (red).

For the linear-to-circular polarizer, two pieces of $20 \times 20 \text{ cm}^2$ substrate patterned with periodic ELC structures were fabricated and fixed with 3.25 mm spacing. The reflection and transmission waves were measured using a pair of X-band lens antennas connected to the vector network analyzer (Rohde and Schwarz ZVA40). On each substrate there are 48×48 ELC unit cells. The electric field of the transmitting antenna is polarized to the direction p1 illustrated in Fig. 1(a), which has a 45° angle with respect to the vertical direction so that the electric fields of the two modes for incident waves are related by $|E_x| = |E_y|$ and $\arg(E_x) = \arg(E_y)$. A calibration was conducted by removing the sample and having the receiving antenna aligned at the same direction with the transmitting antenna, which is marked as 45° . Then we rotated the receiving antenna from 0° to 315° by a step of 45° to achieve the polarization pattern of the incident waves. The comparison of polarization patterns from the measurement and theoretical prediction is shown in Fig. 2(a) for the incident wave at the frequency of 10 GHz.

Afterward we put the sample in between the antenna pairs and measured the polarization pattern of the transmitted waves likewise. The comparison of polarization patterns from the measurement and the theoretical prediction is shown in Fig. 2(b). For circular polarization, the amplitude of electric field is supposed to be invariant (see the gray dotted line) and in our measurement the variation is less than 1 dB. Besides, the phase distribution changes linearly along the circle as expected. Figure 3 compares the simulated and measured transmissions from the incident polarization (p1) to the same polarization direction (p1) and to its cross polarization (p2). Here, p1 and p2 are defined in Fig. 1(a). Over the frequency range around 10 GHz, the field intensity in the two polarization directions are roughly equal to each other at about -3 dB , indicating a full conversion to circular polarization. The frequency dispersion of the polarizer agrees well with the simulation despite the fabrication factor and random error in measurements.

A similar measurement was conducted for a linear-to-linear polarizer with four pieces of the structures of the same ELC pattern. The polarization pattern of the transmitted waves at 10 GHz is shown in Fig. 2(c). Comparing Figs. 2(a) and 2(c), the electric field is rotated by 90° , which marks the

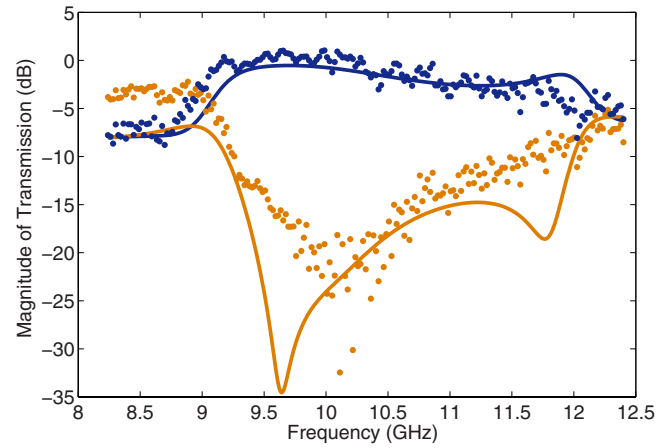


FIG. 4. (Color online) The simulated (solid lines) and measured (dots) transmission of electric fields from p1 to p1 (yellow) and from p1 to p2 (blue).

conversion to the cross polarization of the incident waves. Polarization isolation here is better than -20 dB . Figure 4 compares the simulated and measured transmissions from p1 to p1 and from p1 to p2. Over the frequency range around 10 GHz, it is observed that the field intensity of the cross polarization is close to 0 dB and that of the original polarization is less than -20 dB , which is a direct evidence of small loss and little reflections of the polarizer. We remark that both measurement results are reciprocal.

In conclusion, we reported an experimental demonstration of a metamaterial transmission polarizer based on the accurate design of anisotropic metamaterials. In the experiment, highly efficient conversions from a linear polarization to a circular polarization and to its cross linear polarization have been accomplished. The metamaterial polarizer can manipulate polarization states in many other situations and will find broad applications in various radio frequency and optical devices.

This work was supported in part by the National Science Foundation of China under Grant Nos. 60871016 and 60671015, in part by the Natural Science Foundation of Jiangsu Province under Grant No. BK2008031, in part by the National Basic Research Program (973) of China under Grant No. 2004CB719802, and in part by the 111 Project under Grant No. 111-2-05. J.Y.C. acknowledges support from the foundation for Excellent Doctoral Dissertation of Southeast University under Grant No. 1104000133.

¹D. R. Smith, W. J. Padilla, C. C. Vier, S. C. Nemat-Nasser, and S. Schultz, *Phys. Rev. Lett.* **84**, 4184 (2000).

²J. B. Pendry, D. Schurig, and D. R. Smith, *Science* **312**, 1780 (2006).

³Q. Cheng, R. Liu, J. J. Mock, T. J. Cui, and D. R. Smith, *Phys. Rev. B* **78**, 121102 (2008).

⁴J. Hao, Y. Yuan, L. Ran, T. Jiang, J. A. Kong, C. T. Chan, and L. Zhou, *Phys. Rev. Lett.* **99**, 063908 (2007).

⁵J. Y. Chin, M. Lu, and T. J. Cui, Proceedings of the IEEE-AP/S International Symposium & URSI Radio Science Meeting, 2008 (unpublished).

⁶D. Schurig, J. J. Mock, and D. R. Smith, *Appl. Phys. Lett.* **88**, 041109 (2006).

⁷W. J. Padilla, M. T. Aronsson, C. Highstrete, M. Lee, A. J. Taylor, and R. D. Averitt, *Phys. Rev. B* **75**, 041102 (2007).

⁸D. R. Smith, D. Schultz, P. Markos, and C. M. Soukoulis, *Phys. Rev. B* **65**, 195104 (2002).